A Hybrid Fuzzy Decentralized Sliding Mode Under-actuated Control for Autonomous Dynamic Balance of a Running Electrical Bicycle Including Frictional Torque and Motor Dynamics and in the Presence of Huge Uncertainty

Chih-Lyang Hwang, *Senior Member*, Hsiu-Ming Wu, *Member* and Ching-Long Shih, *Member IEEE*

***Abstract* --- Hybrid under-actuated control for the autonomous dynamic balance of a running electrical bicycle including frictional torque and motor dynamics is developed, where includes two control inputs: steering and pendulum voltages, and three system outputs: steering, lean and pendulum angles. Due to the under-actuated feature, two novel reference signals using three system outputs are designed so that the number of control inputs and sliding surfaces is the same. The previous fuzzy decentralized sliding mode under-actuated control (FDSMUC) is first designed. Because the uncertainties of a running electrical bicycle system, caused by different ground conditions, gusts of wind, and interactions among subsystems, are often huge, an extra compensation of learning uncertainty is plunged into FDSMUC to enhance the system performance. We call it as "fuzzy decentralized sliding mode adaptive under-actuated control (FDSMAUC)." To avoid the unnecessary transience caused by uncertainties and control signal and to preserve the balance of the bicycle, the combination of FDSMUC and FDSMAUC with a transition (i.e., Hybrid FDSMUC) is designed. Finally, the compared simulations for the suggested control system among the FDSMUC, FDSMAUC and Hybrid FDSMUC validate the efficiency of the proposed method.**

1. INTRODUCTION

Under-actuated control has been discussed in some papers. In the past, a nonlinear control scheme for an under-actuated acrobot has been constructed by Berkemeier and Fearing [1]. In fact for the trajectory of 1 *Hz*, no tracking error was committed by their controller, as opposed to the tracking error of 13° by the pseudolinearizing controller. Recently, a paper developed by Yamaguchi et al. using acceleration based backstepping control [2] confirmed that a nonlinear control for an electrical bicycle is better than that of conventional control. Summing up the conclusion reached by previous works, the control of a bicycle's center of gravity (CG) and steering handle angle are two of the most important issues in realizing a stable running motion. In these situations, it is difficult for an electrical bicycle to obtain autonomous dynamic balance when it is in face with huge uncertainties, e.g., varying ground conditions and external disturbances in the air. It is also known that the experimental study of the dynamic balance of a bicycle is not an easy task. In order to consider bicycle system model completely, the inclusion of the frictional torque and motor dynamics is necessary. However, it forms a high dimensional model such that the controller design is more complex. Under these circumstances, the proposed Hybrid FDSMUC for a running electrical bicycle with frictional torque and motor dynamics (i.e., the proposed running electrical bicycle system) and huge uncertainty is applied to deal with exactly what linear control schemes couldn't.

In this paper, a FDSMC scheme with the number of outputs larger than that of the control inputs [3], including FDSMUC, FDSMAUC and Hybrid FDSMUC. The use of FDSMUC or FDSMAUC or Hybrid FDSMUC is dependent on the quantity of the uncertainty including all kind of initial errors, different ground conditions, and gust of wind. Due to the under-actuated feature of an electrical bicycle, two novel reference signals are first designed so that the uncontrolled mode (i.e., the angle, velocity and acceleration of lean) is simultaneously included into these two control modes (i.e., the angle, velocity and acceleration of steering handle and pendulum). Hence, the uncontrolled mode is indirectly manipulated by these two controllable modes. Two sliding surfaces are obtained from the linear combination of these two reference inputs. Then, the theorems about bounded- input-bounded-output (BIBO) and asymptotical tracking for the sliding surface are discussed. According to the previous paper [3], the fuzzy decentralized sliding-mode under-actuated control (FDSMUC) is first designed. Owing to the existence of huge uncertainty for a running electrical bicycle, the fuzzy decentralized sliding-mode adaptive under-actuated control (FDSMAUC) is suggested to enhance the system performance. The difference between FDSMAUC and FDSMUC is that an extra compensation based on the learning uncertainty is plunged into FDSMUC. The purpose of this extra compensation is to reduce the uncertainties caused by different ground conditions, pulse disturbance due to wind effects, and interactions among subsystems. The learning law contains e-modification rate and projection to ensure the no-drift and boundedness of learning weight. Furthermore, the proposed control only learns the uncertainty function to promote better performance. That is different from the most previous papers (e.g., [4]) those learn the whole nonlinear functions. In this situation, the learning error becomes large; then it degrades the robust stability and robust performance. To avoid the unnecessary transient response that destroys the dynamic balance, Hybrid FDSMUC (i.e., the combination of FDSMUC and FDSMAUC with a transition, e.g., [5]) is designed. The stability of the closed-loop system is verified

C. L. Hwang is with the Department of Electrical Engineering, Tamkang University, Tamsui, Taipei County, Taiwan (e-mail: clhwang@mail.tku.edu.tw)

H. M. Wu and C. L. Shih are with the Department of Electrical Engineering, National Taiwan University of Science and Technology, Taipei, Taiwan.

978-1-4244-8126-2/10/$26.00 ©2010 IEEE

by Lyapunov stability theory. Finally, the compared simulations considering time- varying uncertainty, in the presence of the pulse disturbance to represent a gust of wind, for the FDSMUC, FDSMAUC and Hybrid FDSMUC are given.

II. SYSTEM MODELING AND PROBLEM FORMULATION

A. Modeling of Running Electrical Bicycle System

In the beginning, the control mechanism of an electrical bicycle in motion is depicted in Fig. 1 of previous paper [3], in which it can be composed of front wheel part and bicycle body with the pendulum part. The dynamic equation of the front wheel part can be derived from Newton-Euler equations and applied toques contain control torque of steering handle, gravity effect, precession effect, trail effect and internal coulomb friction force that are described as equation (A1). In addition, the dynamic equations (A2) and (A3) can be obtained for a bicycle body with forward speed as well as a pendulum for balancing. In order to consider system more practically and completely, the frictional torques of steering handle and pendulum (i.e., (A4) and (A5)) and the dynamics of armature-controlled dc motors (i.e., (A6) and (A7)) are also included, which is different from the previous paper [3]. Then the original 6th order system becomes an 8th order system.

$$\dot{x}_1(t) = x_4(t) = a_1(x) \tag{1a}$$

$$\dot{x}_2(t) = x_5(t) = a_2(x) \tag{1b}$$

$$\dot{x}_3(t) = x_6(t) = a_3(x) \tag{1c}$$

$$\begin{aligned}\dot{x}_4(t) &= \left\{ f\ mg\sin x_2(t) + I_w \omega\, x_5(t) - \left[C_t x_2(t) t_r \cos x_1(t) \right.\right. \\ &\left.\left. + \mu\ \omega\, t_r \sin x_1(t) \right] + \tau_{han}(t) - F_{f_1}(x_4) \right\} \Big/ I_h \\ &= a_4'(x) + b_4'(x)\tau_{han}(t) = a_4(x)\end{aligned} \tag{1d}$$

$$\begin{aligned}\dot{x}_5(t) &= \left\{ -\left(M_p l_2^2 + M_p l_1 l_2 \cos x_3(t) + J_2\right)\left(M_p l_1 l_2 x_5^2 \sin x_3(t)\right) \right. \\ &+ \left(2M_p l_1 l_2 x_5(t) x_6(t) \sin x_3(t)\right)\left(M_p l_2^2 + J_2\right) \\ &+ \left(M_p l_2^2 + M_p l_1 l_2 \cos x_3(t) + J_2\right)\left(M_p g l_2 \sin\left(x_3(t) - x_2(t)\right)\right) \\ &- \left(M_p l_1 l_2 x_6^2(t) \sin x_3(t)\right)\left(M_p l_2^2 + J_2\right) \\ &+ \left(M_p l_2^2 + M_p l_1 l_2 \cos x_3(t) + J_2\right) \\ &\left[M_p l_2 \cos\left(x_3(t) - x_2(t)\right)\left(V^2 x_1(t) + L_1 V x_4(t)\right) \Big/ L \right] \\ &+ \left(M_b g h \sin x_2(t)\right)\left(M_p l_2^2 + J_2\right) + \left(M_p g l_1 \sin x_2(t)\right)\left(M_p l_2^2 + J_2\right) \\ &+ \left(M_p g l_2 \sin\left(x_3(t) - x_2(t)\right)\right)\left(M_p l_2^2 + J_2\right) \\ &- \left[M_b l_1 \cos x_2(t) + M_p l_2 \cos x_2(t) + M_p l_2 \cos\left(x_3(t) - x_2(t)\right) \right] \\ &\left(V^2 x_1(t) + L_1 V x_4(t)\right)\left(M_p l_2^2 + J_2\right) \Big/ L \\ &\left. + \left(M_p l_2^2 + M_p l_1 l_2 \cos x_3(t) + J_2\right)\left(\tau_{pen}(t) - F_{f_2}(x_6)\right) \right\} \Big/ F(x_2, x_3) \\ &= a_5'(x) + b_5'(x)\tau_{pen}(t) = a_5(x)\end{aligned} \tag{1e}$$

$$\begin{aligned}\dot{x}_6(t) &= \left\{ \left(M_b h^2 + M_p l_1^2 + M_p l_2^2 + 2M_p l_1 l_2 \cos x_3(t) + J_1 + J_2\right) \right. \\ &\cdot \left(M_p l_1 l_2 x_5^2(t) \sin x_3(t)\right) - \left(M_p l_2^2 + M_p l_1 l_2 \cos x_3(t) + J_2\right) \\ &\cdot \left(2M_p l_1 l_2 x_5(t) x_6(t) \sin x_3(t)\right) \\ &- \left(M_b h^2 + M_p l_1^2 + M_p l_2^2 + 2M_p l_1 l_2 \cos x_3(t) + J_1 + J_2\right) \\ &\cdot \left(M_p g l_2 \sin\left(x_3(t) - x_2(t)\right)\right) - \left(M_p l_1 l_2 x_6^2 \sin x_3(t)\right) \\ &\cdot \left(M_p l_2^2 + M_p l_1 l_2 \cos x_3(t) + J_2\right) \\ &- \left(M_b h^2 + M_p l_1^2 + M_p l_2^2 + 2M_p l_1 l_2 \cos x_3(t) + J_1 + J_2\right) \\ &\cdot M_p l_2 \cos\left(x_3(t) - x_2(t)\right)\left(V^2 x_1(t) + L_1 V x_4(t)\right) \Big/ L \\ &- \left(M_b g h \sin x_2(t)\right)\left(M_p l_2^2 + M_p l_1 l_2 \cos x_3(t) + J_2\right) \\ &- \left(M_p g l_1 \sin x_2(t)\right)\left(M_p l_2^2 + M_p l_1 l_2 \cos x_3(t) + J_2\right) \\ &+ \left(M_p g l_2 \sin\left(x_3(t) - x_2(t)\right)\right)\left(M_p l_2^2 + M_p l_1 l_2 \cos x_3(t) + J_2\right) \\ &+ \left[M_b l_1 \cos x_2(t) + M_p l_2 \cos x_2(t) + M_p l_2 \cos\left(x_3(t) - x_2(t)\right) \right] \\ &\cdot \left(V^2 x_1(t) + L_1 V x_4(t)\right)\left(M_p l_2^2 + M_p l_1 l_2 \cos x_3(t) + J_2\right) \Big/ L \\ &- \left(M_b h^2 + M_p l_1^2 + M_p l_2^2 + 2M_p l_1 l_2 \cos x_3(t) + J_1 + J_2\right) \\ &\left. \cdot \left(\tau_{pen}(t) - F_{f_2}(x_6)\right) \right\} \Big/ G(x_3) = a_6'(x) + b_6'(x)\tau_{pen}(t) = a_6(x)\end{aligned} \tag{1f}$$

$$\begin{aligned}\dot{x}_7(t) &= \left\{ -R_1 x_7(t) - K_{b_1} N_1 x_4(t) + u_1(t) \right\} \Big/ \bar{L}_1 \\ &= a_7(x) + b_1 u_1(t)\end{aligned} \tag{1g}$$

$$\begin{aligned}\dot{x}_8(t) &= \left\{ -R_2 x_8(t) - K_{b_2} N_2 x_6(t) + u_2(t) \right\} \Big/ \bar{L}_2 \\ &= a_8(x) + b_2 u_2(t)\end{aligned} \tag{1h}$$

where

$$\begin{aligned}\tau_{han}(t) &= N_1 K_{t_1} x_7(t) = \eta_1 x_7(t), \\ \tau_{pen}(t) &= N_2 K_{t_2} x_8(t) = \eta_2 x_8(t)\end{aligned} \tag{1i}$$

$$\begin{aligned}F(x_3) &= \left(M_b h^2 + M_p l_1^2 + M_p l_2^2 + 2M_p l_1 l_2 \cos x_3(t) + J_1 + J_2\right) \\ &\cdot \left(M_p l_2^2 + J_2\right) - \left(M_p l_2^2 + M_p l_1 l_2 \cos x_3(t) + J_2\right)^2\end{aligned} \tag{1j}$$

$$G(x_3) = -F(x_3). \tag{1k}$$

The states are $x_1(t) = \theta(t)$, $x_2(t) = \phi_1(t)$, $x_3(t) = \phi_2(t)$, $x_4(t) = \dot{\theta}(t)$, $x_5(t) = \dot{\phi}_1(t)$, $x_6(t) = \dot{\phi}_2(t)$, $x_7(t) = i_1(t)$, and $x_8(t) = i_2(t)$. The corresponding variables are explained as follows: $\theta(t), \phi_1(t)$ and $\phi_2(t)$ denote the steering, lean, and pendulum angles, respectively; $i_1(t)$ and $i_2(t)$ are the armature current of DC motors; $\tau_{han}(t)$ and $\tau_{pen}(t)$ respectively represent the steering handle and pendulum torques; $F_{f_1}(x_4)$ and $F_{f_2}(x_6)$ are respectively the steering handle and pendulum frictional torques; $u_1(t)$ and $u_2(t)$ respectively represent the control inputs of the steering and pendulum voltages; the other system parameters are expressed in the Table I. Or, the corresponding matrix form with uncertainty is written as follows:

$$\dot{x}(t) = a(x) + Bu(t) + c(x,t) \tag{2}$$

where $x(t) = \left[x_1(t)\ \ x_2(t)\ \ x_3(t)\ \ x_4(t)\ \ x_5(t)\ \ x_6(t)\ \ x_7(t)\ \ x_8(t) \right]^T$ represents the system state which is available; $a(x) = \left[a_1(x)\ \ a_2(x)\ \ a_3(x)\ \ a_4(x)\ \ a_5(x)\ \ a_6(x)\ \ a_7(x)\ \ a_8(x) \right]^T$ which denotes a mapping from $\Re^8 \to \Re^8$;

$B = \begin{bmatrix} 0 & 0 & 0 & 0 & 0 & 0 & 0 & b_2 \\ 0 & 0 & 0 & 0 & 0 & 0 & b_1 & 0 \end{bmatrix}^T \in \Re^{8\times 2}$ denotes the control gain; $u(t) = [u_1(t) \;\; u_2(t)]^T \in \Re^2$ denotes the control input; $c(x,t)$ denotes the nonlinear time-varying uncertainty caused by the parameter variations, e.g., $\Delta a_i(x,t)$, $i = 4,5,...,8$, $\Delta b_1(t)$ and $\Delta b_2(t)$ in a multiplicity form, or other unmodeled dynamics.

B. Problem Formulation

Because the motion of an electrical bicycle system is often in different operating conditions (e.g., concrete ground, muddy ground, wet ground, different tire pressures, and in the face of a gust of wind), the dynamics of an electrical bicycle is nonlinear, time variant and unstable ([2], [3]). In this paper, it is assumed that the controlled system, i.e., $a(x)$, B, and $c(x,t)$, is unknown. However, the upper bounds of these functions are known.

The three steps for the proposed controller design are described as follows: Firstly, the FDSMUC, which is based on the upper bounds of $a(x)$, B, and $c(x,t)$, is designed such that the outputs exponentially converge into a bounded set of zero, and that the dynamic balance of a running electrical bicycle system is assured [3]. Because the running electrical bicycle is in the presence of huge uncertainty, the FDSMUC is possibly not enough to deal with this situation. Secondly, the FDSMAUC, which is based on the low bounds of $b_{1a}(x) = b_4'(x)\eta_1 b_1 > b_{1al} > 0$, $b_{2a}(x) = b_6'(x)\eta_2 b_2 > b_{2al} > 0$ for all $x(t)$, and the learning laws for the uncertainties, is designed with an extra compensation of uncertainty. Under the subjection of huge uncertainty, the outputs exponentially converge into a bounded set of zero, and the dynamic balance of a running electrical bicycle system in the presence of huge uncertainty is guaranteed. To prevent the unnecessary transience and preserve the dynamic balance, the combination of FDSMUC and FDSMAUC with a transition (i.e., Hybrid FDSMUC) is finally designed such that the outputs exponentially and *smoothly* converge into a bounded set of zero, and that the corresponding autonomous dynamic balance is obtained (see Fig. 1).

III. SLIDING SURFACE FOR UNDER-ACUATED CONTROL SYSTEM

Considering that proposed architecture is an under-actuated control system, the following two sliding surfaces are first defined.

$$s_1(t) = d_{1a}(\ddot{r}_1(t) - \dot{x}_4(t)) + d_{1v}\left(\dot{r}_1(t) - x_4(t)\right) + d_{1p}\left(r_1(t) - x_1(t)\right) \quad (3)$$

$$s_2(t) = d_{2a}(\ddot{r}_3(t) - \dot{x}_6(t)) + d_{2v}\left(\dot{r}_3(t) - x_6(t)\right) + d_{2p}\left(r_3(t) - x_3(t)\right) \quad (4)$$

where $d_{1a}, d_{1v}, d_{1p}, d_{2a}, d_{2v}, d_{2p} > 0$ are set to obtain two stable sliding surfaces $s_1(t)$ and $s_2(t)$, and the reference inputs $r_1(t)$ and $r_3(t)$ are assigned as follows:

$$r_1(t) = k_{1v}\left(\dot{r}_2(t) - x_5(t)\right) + k_{1p}\left(r_2(t) - x_2(t)\right) \quad (5)$$

$$r_3(t) = k_{2v}\left(\dot{r}_2(t) - x_5(t)\right) + k_{2p}\left(r_2(t) - x_2(t)\right) \quad (6)$$

where $k_{1v}, k_{1p}, k_{2v}, k_{2p} > 0$ are set to obtain two stable reference inputs $r_1(t)$ and $r_3(t)$. The reason to design

Table I PARAMETERS OF THE ELECTRICAL BICYCLE.

Parameters	Description	Values
M_b	Mass of electrical bicycle	52.0 kg
m	Mass of front wheel part	10.0 kg
M_p	Mass of inverted pendulum	2.0 kg
L	Wheel base	1.13 m
L_1	CG position from rear wheel	0.324 m
L_2	CG position from front wheel	0.806 m
h	Height of CG	0.855 m
l_1	Height of the axis of pendulum	1.0 m
l_2	Length of pendulum	0.51 m
r	Radius of wheel	0.35 m
V	Speed of bicycle	3.0 m/s
f	Offset	0.06 m
t_r	Trail	0.05 m
I_h	Inertial of front wheel about handle axis	0.35 kgm^2
I_w	Inertial of wheel	0.18 kgm^2
μ	Coefficient of conflict	0.1
J_1	Inertial of CG about x axis	10.0 kgm^2
J_2	Inertial of inverted pendulum	0.0463 kgm^2
C_t	Coefficient of camber thrust	66.0 N/rad
$\bar{L}_1, \bar{L}_2$	Inductances of the armature circuit	0.048 H
R_1, R_2	Resistances of the armature circuit	1.6 Ω
K_{b_1}, K_{b_2}	Back EMF constants of the motor	0.19 V/(rad/s)
N_1, N_2	Gear ratio	63,108
K_{t_1}, K_{t_2}	Motor torque constants	0.2613 Nm/A

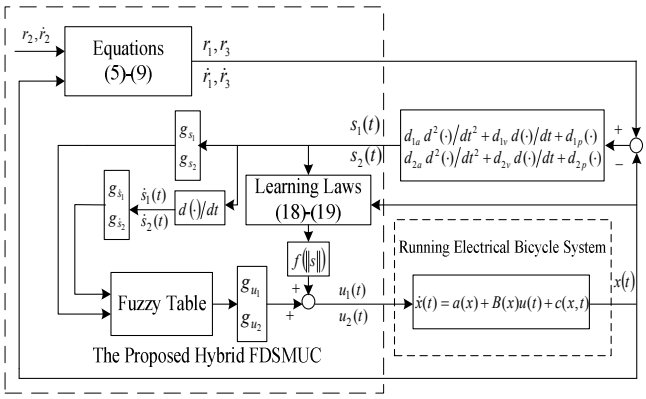

Fig. 1. Control block diagram of the overall system.

these reference signals of (5) and (6) is that the uncontrolled mode $x_2(t)$ and $x_5(t)$ should be simultaneously included into the two control modes (i.e., $x_1(t), x_3(t)$ or $x_4(t), x_6(t)$) so that they are indirectly manipulated by these controllable modes. In this paper, $r_2(t) = \dot{r}_2(t) = \ddot{r}_2(t) = 0$ is considered. For simplicity, the tracking error is defined as follows:

$$e_i(t) = r_i(t) - x_i(t), \dot{e}_i(t) = e_{i+3}(t), i = 1,2,3. \quad (7)$$

. Based on (2), (5) and (6), the following equations are obtained.

$$\begin{aligned}\dot{r}_1(t) &= k_{1v}\left(\ddot{r}_2(t) - \dot{x}_5(t)\right) + k_{1p}\left(\dot{r}_2(t) - \dot{x}_2(t)\right) \\ &= k_{1v}\left[\ddot{r}_2(t) - a_5(x) - c_5(x,t)\right] + k_{1p}\left(\dot{r}_2(t) - x_5(t) - c_2(x,t)\right)\end{aligned} \quad (8)$$

$$\begin{aligned}\dot{r}_3(t) &= k_{2v}\left(\ddot{r}_2(t) - \dot{x}_5(t)\right) + k_{2p}\left(\dot{r}_2(t) - \dot{x}_2(t)\right) \\ &= k_{2v}\left[\ddot{r}_2(t) - a_5(x) - c_5(x,t)\right] + k_{2p}\left(\dot{r}_2(t) - x_5(t) - c_2(x,t)\right).\end{aligned} \quad (9)$$

Remark 2: Because the system functions are unknown, the signals $\dot{r}_1(t)$ and $\dot{r}_3(t)$ in (8) and (9) are approximate by $\Delta r_1(n)$ and $\Delta r_3(n)$, where $\Delta r_1(n) = \left[r_1(n) - r_1(n-1)\right]/T_s$, $\Delta r_3(n) = \left[r_3(n) - r_3(n-1)\right]/T_s$, T_s is the sampling time, and $r_1(n), r_3(n)$ denote the *nth* time interval of $r_1(t), r_3(t)$, which are obtained from the equations (5) and (6). Through the verification of the computer simulation, the similar responses are obtained. It also can be thought as an uncertainty.

Then the derivatives of these two sliding surfaces are

$$\begin{aligned}\dot{s}_1 &= d_{1a}\left(\dddot{r}_1(t) - \dddot{x}_4(t)\right) + d_{1v}\left(\ddot{r}_1(t) - \ddot{x}_4(t)\right) + d_{1p}\left(\dot{r}_1(t) - x_4(t)\right) \\ &= d_{1a}\left(\dddot{r}_1(t) - \rho_1(x) - b_{1a}(x)u_1(t)\right) + d_{1v}\left(\ddot{r}_1(t) - a_4'(x)\right. \\ &\left. - b_4'(x)\eta_1 x_7(t) - c_4(x,t)\right) + d_{1p}\left(\dot{r}_1(t) - x_4(t) - c_1(x,t)\right)\end{aligned} \quad (10)$$

$$\begin{aligned}\dot{s}_2 &= d_{2a}\left(\dddot{r}_3(t) - \dddot{x}_6(t)\right) + d_{2v}\left(\ddot{r}_3(t) - \ddot{x}_6(t)\right) + d_{2p}\left(\dot{r}_3(t) - x_6(t)\right) \\ &= d_{2a}\left(\dddot{r}_3(t) - \rho_2(x) - b_{2a}(x)u_2(t)\right) + d_{2v}\left(\ddot{r}_3(t) - a_6'(x)\right. \\ &\left. - b_6'(x)\eta_2 x_8(t) - c_6(x,t)\right) + d_{2p}\left(\dot{r}_3(t) - x_6(t) - c_3(x,t)\right)\end{aligned} \quad (11)$$

where $c_i(x,t), i = 1,2,...,8$, denote the *ith* component of $c(x,t)$, $b_{1a}(x) = b_4'(x)\eta_1 b_1$, $b_{2a}(x) = b_6'(x)\eta_2 b_2$ are unknown functions to be learning, and $\rho_1(x) = \rho_{11}(x) + b_4'(x)\eta_1 a_7(x)$, $\rho_2(x) = \rho_{21}(x) + b_6'(x)\eta_2 a_8(x)$, where $\rho_{11}(x) = \dot{a}_4'(x) + \dot{b}_4'(x)\eta_1 x_7(t)$, $\rho_{21}(x) = \dot{a}_6(x) + \dot{b}_6'(x)\eta_2 x_8(t)$. These two terms $\dot{a}_4'(x)$ and $\dot{a}_6'(x)$ can be respectively obtained from time derivative of (1d) and (1f). For simplicity, those are omitted.

IV. CONTROLLER DESIGN

The procedure of three-step controller design is respectively discussed in the following three subsections.

A. FDSMUC

The FDSMUC is then designed as follows [3]:

$$u_i(t) = u_{i,FDSMUC}(t) = g_{u_i}\overline{u}_i(t) = g_{u_i}\left[s_i(t) + \Delta_i(t)\,\mathrm{sgn}(s_i)\right] \quad (13)$$

where $\overline{u}_i(t)$ is the fuzzy variable of $u_i(t)$, g_{u_i} denotes the output scaling factor, and $\Delta_i(t) > 0\ \forall t$ denotes the switching gain for $i = 1,2$. The output scaling factors are supposed to satisfy the following inequalities:

$$\begin{aligned}&g_{u_1} \ge \left(\left|h_1(x,t)\right| + \lambda_1\right)\Big/\left(d_{1a}b_{1a}(x)\Delta_1(t)\right), \\ &g_{u_2} \ge \left(\left|h_2(x,t)\right| + \lambda_2\right)\Big/\left(d_{2a}b_{2a}(x)\Delta_2(t)\right), \forall t, x(t)\end{aligned} \quad (14)$$

where $\lambda_1, \lambda_2 > 0$, and

$$\begin{aligned}h_1(x,t) &= d_{1a}\left(\dddot{r}_1(t) - \rho_1(x)\right) + d_{1v}\left[\ddot{r}_1(t) - a_4'(x) - \right. \\ &\left. b_4'(x)\eta_1 x_7(t) - c_4(x,t)\right] + d_{1p}\left(\dot{r}_1(t) - x_4(t) - c_1(x,t)\right)\end{aligned} \quad (15)$$

$$\begin{aligned}h_2(x,t) &= d_{2a}\left(\dddot{r}_3(t) - \rho_2(x)\right) + d_{2v}\left[\ddot{r}_3(t) - a_6'(x) - \right. \\ &\left. b_6'(x)\eta_2 x_8(t) - c_6(x,t)\right] + d_{2p}\left(\dot{r}_3(t) - x_6(t) - c_3(x,t)\right).\end{aligned} \quad (16)$$

Then the properties of the FDSMUC also can refer to the previous paper [3].

B. FDSMAUC

If the system uncertainties (15) or (16), i.e., $h_i(x,t), i = 1,2$, are huge, they must be learned to improve the system performance [5]. In this way,

$$h_i(x,t) = \overline{W}_i^T\Psi(x) + \varepsilon_i(x,t), i = 1,2$$

where $\overline{W}_i \in \Re^{L\times 1}$ is an unknown constant matrix which is not necessarily unique, $\left|\varepsilon_i(x,t)\right| \le \varepsilon\ \ \forall x(t) \in D(x)$ and $t \ge 0$. In addition, the upper bound of $\overline{W}_i$ is known, i.e., $\left\|\overline{W}_i\right\| \le \overline{W}_{im}$. The following learning laws are considered.

$$\dot{\hat{W}}_i(t) = s_i(t)\Gamma_i^{-1}\Psi(x) - \alpha_i\Gamma_i^{-1}\hat{W}_i(t), i = 1,2 \quad (18a)$$

where $\hat{W}_i(t) \in \Re^{L\times 1}$ stands for the learning weight, $\Gamma_i > 0$, $\alpha_i > 0$ denotes an *e*-modification rate to ensure the boundedness of the learning weight, $\Psi(x) \in \Re^{L\times 1}$ denotes the basis function:

$$\Psi(x) = \left[1 \quad \varphi_2(x) \quad ... \quad \varphi_L(x)\right]^T \quad (18b)$$

where $\varphi_j(x) = \exp\left[-\left\|x(t) - d_j\right\|^2\Big/\sigma_j^2\right]$, L, d_j, σ_j for j = 2, 3,…, L are known, and the centers d_j for $j = 2,3,...,L$ are chosen as normal distribution in the corresponding domain. The nonlinear control gains i.e., $b_{1a}(x)$ and $b_{2a}(x)$ are unknown. However, their low bounds are supposed to be known, i.e., $b_{1a}(x) > b_{1al} > 0$ and $b_{2a}(x) > b_{2al} > 0$ for all $x(t)$. Their upper bounds are also supposed to be existed, i.e., $\max\left\{b_{1a}(x)\right\} \le b_{1am}$ and $\max\left\{b_{2a}(x)\right\} \le b_{2am}$ for all $x(t)$. Similarly, the learning laws for $b_{1a}(x)$ and $b_{2a}(x)$ are

$$\begin{aligned}\dot{\hat{b}}_{1a}(t) &= s_1(t)\beta_1^{-1}\psi_1(t) - \Pr\left[\hat{b}_{1a}(t), \alpha_3\beta_1^{-1}\hat{b}_{1a}(t)\right], \\ \dot{\hat{b}}_{2a}(t) &= s_2(t)\beta_2^{-1}\psi_2(t) - \Pr\left[\hat{b}_{2a}(t), \alpha_4\beta_2^{-1}\hat{b}_{2a}(t)\right]\end{aligned} \quad (19a)$$

where $\beta_1, \beta_2, \alpha_3, \alpha_4 > 0$, $\psi_1(t) = -\hat{W}_1^T(t)\psi(x)\big/\hat{b}_{1a}(t)$, $\psi_2(t) = -\hat{W}_2^T(t)\Psi(x)\big/\hat{b}_{2a}(t)$, and

$$\begin{aligned}&\Pr\left[\hat{b}_{ia}(t), \alpha_{i+2}\beta_i^{-1}\hat{b}_{ia}(t)\right] \\ &= \begin{cases}\alpha_{i+2}\beta_i^{-1}\hat{b}_{ia}(t) + \alpha_{i+2}\beta_i^{-1}\left(b_{ial} - \hat{b}_{ia}(t)\right)\Big/\delta_i, & \text{if } \hat{b}_{ia}(t) < b_{ial} \\ \alpha_{i+2}\beta_i^{-1}\hat{b}_{ia}(t), & \text{otherwise}\end{cases}\end{aligned} \quad (19b)$$

where $\delta_1, \delta_2 > 0$. Once $\hat{b}_{1a}(t) < b_{1al}$ or $\hat{b}_{2a}(t) < b_{2al}$ occurs, the projection term in (19b) is employed to ensure that the learning quickly returns to its true region. In this situation, the occurrence of $\hat{b}_{1a}(t)$ or $\hat{b}_{2a}(t)$ approaching zero is avoided. Then the FDSMAUC is designed as

$$u_i(t) = u_{i,FDSMAUC}(t) = g_{u_i}\left[s_i(t) + \Delta_i(t)\,\mathrm{sgn}(s_i)\right] + \hat{W}_i^T(t)\Psi(x)\Big/\left(d_{ia}\hat{b}_{ia}(t)\right), i = 1,2 \quad (20)$$

where $g_{u_1} > \gamma_1 / d_{1a} b_{1a}(x) > 0$, $g_{u_2} > \gamma_2 / d_{2a} b_{2a}(x) > 0$, and $\Delta_i(t) > 0, i = 1,2 \ \forall t$. The small positive constants γ_1 and $\gamma_2 > 0$ are employed to guarantee an exponential tracking to a convex set (22).

Theorem 1: Consider the unknown electrical bicycle system (2) with the known lower bounds of $b_{1a}(x) > b_{1al} > 0$ and $b_{2a}(x) > b_{2al} > 0$ for all $x(t)$. The switching gains $\Delta_1(t)$ and $\Delta_2(t)$ in (20) are selected such that the following inequalities are satisfied.

$$\Delta_1(t) > \left|\varepsilon_1(x,t)\right| \Big/ \left(d_{1a} b_{1a}(x) g_{u_1} - \gamma_1\right),$$
$$\Delta_2(t) > \left|\varepsilon_2(x,t)\right| \Big/ \left(d_{2a} b_{2a}(x) g_{u_2} - \gamma_2\right) \quad (21)$$

If the control law (20) with the learning laws (18) and (19) is applied to the system (2), then $\left\{\hat{W}_1(t), \hat{W}_2(t), \hat{b}_{1a}(t), \hat{b}_{2a}(t), s_1(t), s_2(t), u_1(t), u_2(t)\right\}$ are UUB, and the performance is exponentially converged into the convex set:

$$D_a = \left\{ s(t) \in \Re^2 \;\middle|\; 0 \le \left|s_1(t)\right| \le \theta_1,\ 0 \le \left|s_2(t)\right| \le \theta_2 \right\} \quad (22a)$$

where

$$\theta_i = -f_{i1} + \sqrt{f_{i1}^2 + f_{i2}}, \ i = 1,2 \quad (22b)$$

$$f_{i1} = \left\{\Delta_i(t) - \left|\varepsilon_i(x,t)\right| \Big/ \left(d_{ia} b_{ia}(x) g_{u_i} - \gamma_i\right)\right\} \Big/ 2 > 0,$$
$$f_{i2} = \left\{\alpha_i \left\|\bar{W}_{im}\right\|^2 + \alpha_{i+2} b_{iam}^2\right\} \Big/ \left(2 d_{ia} b_{ia}(x) g_{u_i} - 2\gamma_i\right) > 0, i = 1,2 \quad (22c)$$

Proof: See *Appendix B*.

C. Hybrid FDSMUC

When the operating point is far away from the sliding surface, the learning law generally does not require so that the unnecessary instability and transient response are avoided, and then the dynamic balance can be guaranteed [5]. Although the controller in (20) is superior to that in (13), it is still a question when the learning law should be used. Important index for the sliding-mode control is the sliding surface. Due to the existence of system uncertainties, the operating point is always away from the sliding surface. Based on this knowledge, a scalar function $f\left(\|s\|\right)$, where $\|s\| = \sqrt{s_1^2 + s_2^2}$, is designed as follows. When the norm of the sliding surfaces is inside of a defined set, the learning laws (18) and (19) start; similarly, as it is outside of the other set, the learning laws shut off. For reducing the possibility of discontinuous control input, a transition between the control (13) and the control (20) is consigned. Hence, we design the following scalar function:

$$f\left(\|s\|\right) = \begin{cases} 0, & \text{as } \|s(t)\| > n_{s1} \\ 1, & \text{as } \|s(t)\| < n_{s2} \\ \left(n_{s1} - \|s(t)\|\right) \Big/ \left(n_{s1} - n_{s2}\right), & \text{otherwise} \end{cases} \quad (23)$$

where $n_{s1} > \sqrt{d_{s_1}^2 + d_{s_2}^2} > n_{s2} > \sqrt{c_1^2 + c_2^2} > 0$. The values of $\sqrt{d_{s_1}^2 + d_{s_2}^2}$ and $\sqrt{c_1^2 + c_2^2}$ are respectively the upper bounds of the convergent sets of $\|s(t)\|$ for the FDSMUC and FDSMAUC. Finally, the Hybrid FDSMUC is designed as

$$u_i(t) = u_{i,HYB}(t) = g_{u_i}\left[s_i(t) + \Delta_i(t)\,\mathrm{sgn}(s_i)\right] + f\left(\|s\|\right)\hat{W}_i^T(t)\Psi(x)\Big/\left(d_{ia}\hat{b}_{ia}(t)\right), i = 1,2. \quad (24)$$

V. SIMULATIONS AND DISCUSSIONS

In this paper, $r_2(t) = \dot{r}_2(t) = \ddot{r}_2(t) = 0$, $\dddot{r}_1(t) = \ddddot{r}_1(t) = 0$, $\dddot{r}_3(t) = 0$, and $\ddddot{r}_3(t) = 0$. The coefficients of the sliding surfaces are set as follows: $d_{1v} = 16.0$, $d_{1p} = 90$, $d_{2v} = 13.0$, $d_{2p} = 95$, $k_{1v} = 1.6$, $k_{1p} = 17$, $k_{2v} = 0.5$ and $k_{2p} = 11.8$. The uncertainty of the multiplication form (i.e., $a_i(x)(1 + \Delta a_i(x,t))$, $i = 4,5,\ldots 8$, $b_1(1 + \Delta b_1(x,t))$, and $b_2(1 + \Delta b_2(x,t))$) to represent the $c(x,t)$ is assumed to be:

$$\begin{aligned}
&\Delta a_4(x,t) = 1.5 x_1(t) x_2(t) \sin\left(0.3t\ x_5(t)\right) \\
&-0.37 x_3(t) x_6(t) \cos\left(0.2t\ x_6(t)\right) - 0.2 \sin\left(100\ t\right) \\
&\Delta a_5(x,t) = 1.5 x_2(t) x_3(t) \sin\left(0.3t\ x_6(t)\right) \\
&-0.37 x_1(t) x_4(t) \cos\left(0.1t\ x_5(t)\right) - 0.2 \cos\left(200\ t\right) \\
&\Delta a_6(x,t) = 1.5 x_3(t) x_1(t) \sin\left(0.3t\ x_4(t)\right) \\
&+0.37 x_2(t) x_5(t) \cos\left(0.3t\ x_4(t)\right) + 0.2 \sin\left(300\ t\right) \\
&\Delta a_7(x,t) = 1.0 x_4(t) x_1(t) \sin\left(0.3t\ x_4(t)\right) \\
&+0.37 x_5(t) x_8(t) \cos\left(0.4t\ x_8(t)\right) - 0.2 \sin\left(400\ t\right) \\
&\Delta a_8(x,t) = 1.0 x_5(t) x_3(t) \sin\left(0.3t\ x_4(t)\right) \\
&+0.37 x_6(t) x_7(t) \cos\left(0.5t\ x_7(t)\right) + 0.2 \sin\left(500\ t\right) \\
&\Delta b_1(x,t) = 0.3 \sin\left(-0.1 + 9.6t\ x_3(t)\right) + 0.5 \sin\left(300\ t\right) \\
&\Delta b_2(x,t) = 0.3 \sin\left(0.1 + 6.9t\ x_1(t)\right) - 0.5 \cos\left(100\ t\right).
\end{aligned} \quad (25)$$

This uncertainty is nonlinear time-varying and large. To compare the performances among the FDSMUC, FDSMAUC and Hybrid FDSMUC, the following larger uncertainty as compared with the uncertainty (25) is considered.

$$\begin{aligned}
&\Delta a_4(x,t) = 3.0 x_1(t) x_2(t) \sin\left(0.3t\ x_5(t)\right) \\
&-0.74 x_3(t) x_6(t) \cos\left(0.2t\ x_6(t)\right) - 0.24 \sin\left(100\ t\right) \\
&\Delta a_5(x,t) = 3.0 x_2(t) x_3(t) \sin\left(0.3t\ x_6(t)\right) \\
&-0.74 x_1(t) x_4(t) \cos\left(0.1t\ x_5(t)\right) - 0.24 \cos\left(200\ t\right) \\
&\Delta a_6(x,t) = 3.0 x_3(t) x_1(t) \sin\left(0.3t\ x_4(t)\right) \\
&+0.74 x_2(t) x_5(t) \cos\left(0.3t\ x_4(t)\right) + 0.24 \sin\left(300\ t\right) \\
&\Delta a_7(x,t) = 2.0 x_4(t) x_1(t) \sin\left(0.3t\ x_4(t)\right) \\
&+0.74 x_5(t) x_8(t) \cos\left(0.4t\ x_8(t)\right) - 0.24 \sin\left(400\ t\right) \\
&\Delta a_8(x,t) = 2.0 x_5(t) x_3(t) \sin\left(0.3t\ x_4(t)\right) \\
&+0.74 x_6(t) x_7(t) \cos\left(0.5t\ x_7(t)\right) + 0.24 \sin\left(500\ t\right) \\
&\Delta b_1(x,t) = 0.36 \sin\left(-0.1 + 9.6t\ x_3(t)\right) + 0.6 \sin\left(300\ t\right) \\
&\Delta b_2(x,t) = 0.36 \sin\left(0.1 + 6.9t\ x_1(t)\right) - 0.6 \cos\left(100\ t\right).
\end{aligned} \quad (26)$$

The simulations use the numerical algorithm of the fourth-

order Runge-Kutta with time step 0.01 second. The scaling factors of the FDSMUC are set as follows: $g_{s_1} = 0.03$, $g_{\dot{s}_1} = 0.02$, $g_{u_1} = 10$, $g_{s_2} = 0.01, g_{\dot{s}_2} = 0.02$, and $g_{u_2} = 10$. The parameters of Coulomb friction torque are set as $F_{s_1}^+(F_{s_1}^-) = \pm 0.5$, $F_{s_2}^+(F_{s_2}^-) = \pm 0.5$, $\delta F_1^+(\delta F_1^-) = 0.5(-0.4)$, $\delta F_2^+(\delta F_2^-) = 0.5(-0.4)$, $C_1^+(C_1^-) = 0.1$, $C_2^+(C_2^-) = 0.1$, $\dot{\theta}^+(\dot{\theta}^-) = 0.2(0.16)$, $\chi_1 = \chi_2 = 0.5$ and $\varepsilon = 0.01$. The response for the running electrical bicycle in the presence of the uncertainty (25) by the FDSMUC is shown in Fig. 2. The response of Fig. 2 verifies the better robustness of the proposed FDSMUC for the uncertainty (25). However, the responses of the FDSMUC for huge uncertainty (e.g., the uncertainty (26)) become larger transience or more oscillatory (cf. Fig. 3). It indicates that the performance of the FDSMUC is limited by the quantity of uncertainty. Under this circumstance, the FDSMAUC is considered. The response using the same scaling factors of FDSMUC, and the learning parameters: $\Gamma_1 = diag\{0.03\}$, $\Gamma_2 = diag\{0.04\}$, $\alpha_1 = 0.1, \alpha_2 = 0.1$, $\beta_1 = 3.0$, $\beta_2 = 5.0$, is shown in Fig. 4, which is much better than that of Fig. 3. The main reason is that the corresponding learning uncertainties in Fig. 4(c) and (d) are good enough for the compensation of the uncertainties (the solid lines in Fig. 4(c) and (d)). However, the transient response of the FDSMAUC caused by the initial error of the learning weight occurs. This feature probably destroys the dynamic balance of a running electrical bicycle. In this situation, the Hybrid FDSMUC is suggested to enhance system performance. Based on the norm of the sliding surface (i.e., Fig. 2(c)), the suitable control parameters are selected as follows: $n_{s1} = 50$ and $n_{s2} = 30$. The corresponding response is shown in Fig. 5, which is indeed better than that of the FDSMUC and FDSMAUC (cf. Figs 3(a), 4(a) and 5(a)).

For the consideration of practical situations, the following simulation with the uncertainty (26) is investigated. It is assumed that a gust of wind during the period 4.0~4.1 second brings about the extra effect of the lean angle 6° from 4.0 to 4.1 second. The corresponding results by the FDSMUC, FDSMAUC and Hybrid FDSMUC are then shown in Figs 6 and 7. From these two figures, we know that the resistance of the pulse disturbance by the Hybrid FDSMUC is superior to that of the FDSMUC and FDSMAUC. Then the important observations are depicted as follows: (i)The FDSMAUC can improve the performances of the FDSMUC for a running electrical bicycle system in the presence of huge uncertainty. However, a possible transient response occurs. In this situation, the dynamic balance of a running electrical bicycle may be destroyed. (ii) The proposed Hybrid FDSMUC indeed can enhance the system performance including the transient response and steady-state response; it also possesses excess robustness as compared with the FDSMUC. (iii) The resistance of the pulse disturbance (e.g., a gust of wind) by the Hybrid FDSMUC is better than that of the FDSMUC and FDSMAUC.

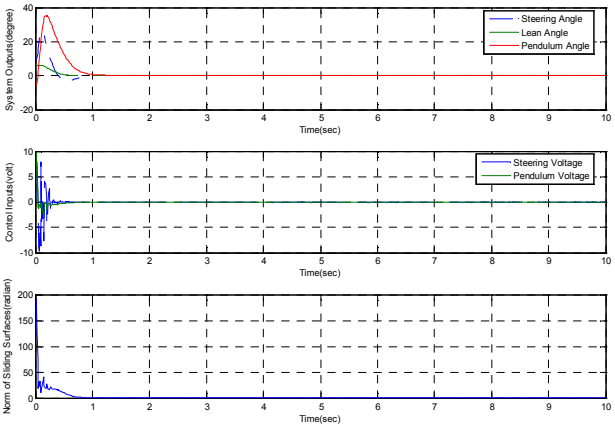

Fig. 2. The responses of the running electrical bicycle with motor dynamics and the uncertainty (26) by the FDSMUC.

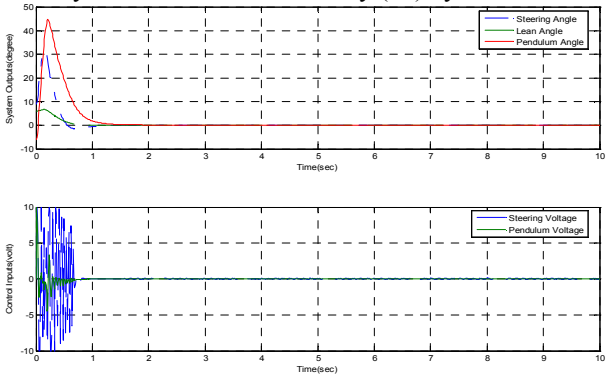

Fig. 3. The responses of the running electrical bicycle with motor dynamics and the huge uncertainty (27) by the FDSMUC.

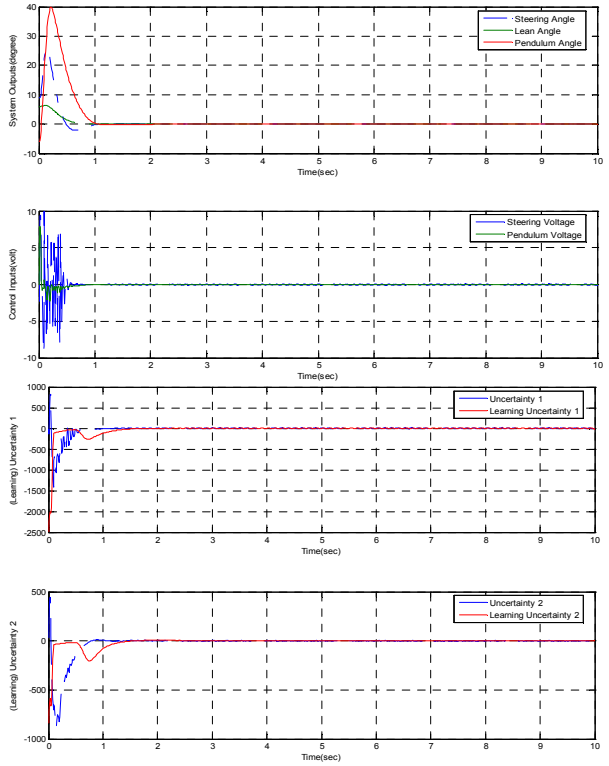

Fig. 4. The responses of the Fig. 3 case by the FDSMAUC.

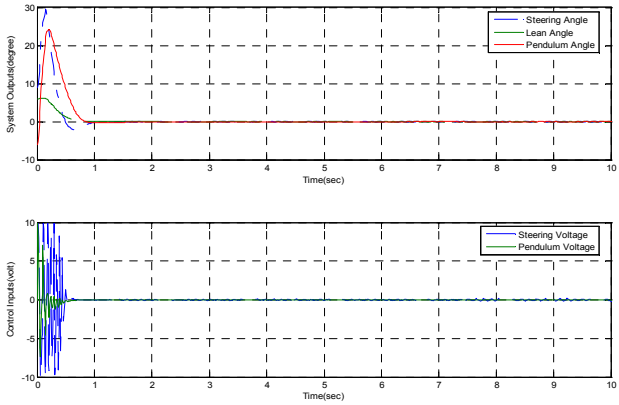

Fig. 5. The responses of the Fig. 3 case by the Hybrid FDSMUC with $n_{s1} = 50$ and $n_{s2} = 30$.

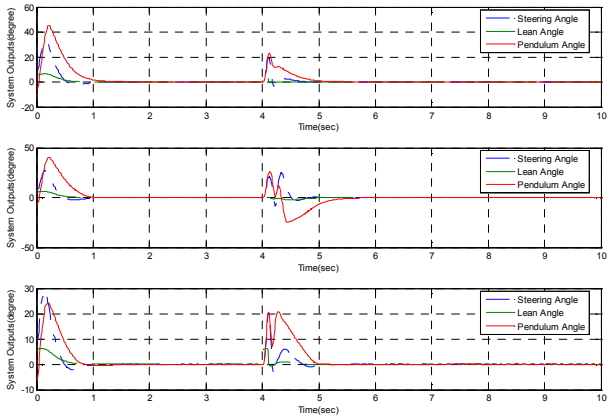

Fig. 6. The output responses of the Fig. 5 case in the face of the pulse disturbance of the lean angle 6.0° from 4.0 to 4.1 second by the FDSMUC, FDSMAUC and Hybrid FDSMUC.

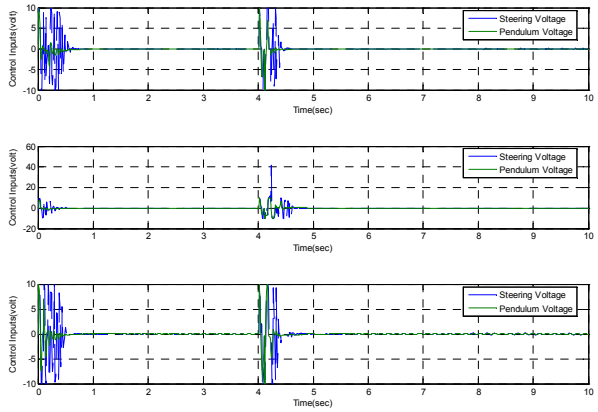

Fig. 7. The control input responses of the Fig. 5 case in the face of the pulse disturbance of the lean angle 6.0° from 4.0 to 4.1 second by the FDSMUC, FDSMAUC and Hybrid FDSMUC.

IV. CONCLUSIONS

The important features of this paper are summarized as follows: (i) The inclusion of frictional torque and motor dynamics is to obtain more complete modeling of a running electrical bicycle. Based on two novel reference inputs, two sliding surfaces are individually obtained. (ii) As the system uncertainty is huge, the Hybrid FDSMUC is applied to improve system performance. Its corresponding control parameters are obtained according to that of the FDSMUC and FDSMAUC. To avoid the unnecessary instability and transient response, the Hybrid FDSMUC is suggested. (iii) The system performances, including the tracking performance for nonlinear time-varying uncertainty, generation of pulse disturbance to simulate wind effects, are acceptable for the FDSMUC, FDSMAUC, and Hybrid FDSMUC. In terms of the transient response and excess robustness, the performance of the Hybrid FDSMUC for huge uncertainty is better than that of the FDSMUC and FDSMAUC.

Acknowledgement: The second and the third authors would like to appreciate the financial support from National Council of Science of R.O.C. with Grant No. NSC-98-2221-E-011-078.

REFERENCES

[1] M. D. Berkemeier and R. S. Fearing, "Tracking fast inverted trajectories of the underactuated acrobot," *IEEE Trans. Robotics & Automat.*, vol. 15, no. 4, pp. 740-750, Aug. 1999.

[2] T. Yamaguchi, T. Shibata and T. Murakami, "Self-sustaining approach of electrical bicycle by acceleration control based backstepping," 33rd *Annual Conference of IEEE IECON*, Taipei, Taiwan, pp. 2610-2613, Nov. 5th-8th, 2007.

[3] C. L. Hwang, H. M. Wu, and C. L. Shih, "Fuzzy sliding-mode under-actuated control for autonomous dynamic balance of an electrical bicycle," *IEEE Trans. Control Syst. Technol.*, vol. 15, no. 3, pp. 658-670, May 2009.

[4] D. Zhang, L. F. Deng, K. Y. Cai and A. So, "Fuzzy nonlinear regression with fuzzified radial basis function network," *IEEE Trans. Fuzzy Syst.*, vol. 13, no. 6, pp. 742-760, Dec. 2005.

[5] C. L. Hwang, "A novel Takagi-Sugeno-based robust adaptive fuzzy sliding mode controller," *IEEE Trans. Fuzzy Syst.*, vol. 12, no. 5, pp. 676-687, Oct. 2004.

APPENDIXES

Appendix A (*The dynamics of the electrical bicycle including frictional torque and motor dynamics*):

The front wheel part:

$$I_h\ddot{\theta} = \tau_{han} + fmg\sin\phi_1 + I_w\omega\dot{\phi}_1 - \left(C_t\phi_1 t_r\cos\theta + \mu\omega t_r\sin\theta\right) - F_{f_1}(\dot{\theta}) \quad \text{(A1)}$$

The bicycle body with the pendulum part:

$$\left(M_b h^2 + M_p l_1^2 + M_p l_2^2 + 2M_p l_1 l_2\cos\phi_2 + J_1 + J_2\right)\ddot{\phi}_1 - \left(M_p l_2^2 + M_p l_1 l_2\cos\phi_2 + J_2\right)\ddot{\phi}_2 - 2M_p l_1 l_2\sin\phi_2\dot{\phi}_1\dot{\phi}_2 + M_p l_1 l_2\sin\phi_2\dot{\phi}_2^2 - M_b gh\sin\phi_1 - M_p gl_1\sin\phi_1 + M_p gl_2\sin\left(\phi_2 - \phi_1\right) + \left(M_b l_1\cos\phi_1 + M_p l_2\cos\phi_1 + M_p l_2\cos\left(\phi_2 - \phi_1\right)\right) \cdot\left(V^2\theta + L_1 V\dot{\theta}\right)/L = 0 \quad \text{(A2)}$$

$$-\left(M_p l_2^2 + M_p l_1 l_2\cos\phi_2 + J_2\right)\ddot{\phi}_1 + \left(M_p l_2^2 + J_2\right)\ddot{\phi}_2 + M_p l_1 l_2\sin\phi_2\dot{\phi}_1^2 - M_p gl_2\sin\left(\phi_2 - \phi_1\right) - M_p l_2\cos\left(\phi_2 - \phi_1\right)\left(V^2\theta + L_1 V\dot{\theta}\right)/L = \tau_{pen} - F_{f_2}(\dot{\phi}_2) \quad \text{(A3)}$$

where $F_{f_i}(\cdot), i = 1,2$ including sticking and slipping torques:

$$F_{f_i}(\cdot) = F_{slip_i}(\cdot)\rho(\cdot) + F_{stick_i}(u_i)\left[1 - \rho(\cdot)\right], i = 1,2, \quad \text{(A4)}$$

where $\rho(\cdot) = 1$ as $\left|\dot{\theta}(\cdot)\right| > \varepsilon$, and $\rho(\cdot) = 0$, otherwise.

$$F_{stick_i}(u_i)=\begin{cases} F_{s_i}^{+} & u_i/\chi_i > F_{s_i}^{+} > 0 \\ u_i/\chi_i & F_{s_i}^{-} \le u_i/\chi_i \le F_{s_i}^{+} \\ F_{s_i}^{-} & u_i/\chi_i < F_{s_i}^{-} < 0 \end{cases}, \quad \text{(A5)}$$

$$F_{slip_i}(\dot{\theta})=\begin{cases} F_{k_i}^{+}(\dot{\theta})=F_{s_i}^{+}-\delta F_i^{+}\left\{1-\exp\left[-\left|\dot{\theta}/\dot{\theta}^{+}\right|\right]\right\}+C_i^{+}\dot{\theta},\ \dot{\theta}>0 \\ F_{k_i}^{-}(\dot{\theta})=F_{s_i}^{-}-\delta F_i^{-}\left\{1-\exp\left[-\left|\dot{\theta}/\dot{\theta}^{-}\right|\right]\right\}+C_i^{-}\dot{\theta},\ \dot{\theta}\le 0 \end{cases}$$

The relation between dynamics of armature-controlled dc motors at the electrical bicycle system and applied torques of steering handle and pendulum is respectively is described as follows:

$$\bar{L}_1\dot{i}_1+R_1 i_1+K_{b_1}\dot{\theta}_m=u_1,\ \bar{L}_2\dot{i}_2+R_2 i_2+K_{b_2}\dot{\phi}_m=u_2 \quad \text{(A6)}$$

where $\theta_m=N_1\theta,\ \phi_m=N_2\phi_2$. The torques of steering handle and pendulum at the joint side are related to the armature currents by

$$\tau_{han}=N_1K_{t_1}i_1,\ \tau_{pen}=N_2K_{t_2}i_2. \quad \text{(A7)}$$

Appendix B (*The proof of Theorem 3*):

First, the following Lyapunov function is defined.

$$V=\left\{s_1^2+s_2^2+\tilde{W}_1^T\Gamma_1\tilde{W}_1+\tilde{W}_2^T\Gamma_2\tilde{W}_2+\beta_1\tilde{b}_{1a}^2+\beta_2\tilde{b}_{2a}^2\right\}/2 \quad \text{(B1)}$$

where $\tilde{W}_1=\bar{W}_1-\hat{W}_1,\tilde{W}_2=\bar{W}_2-\hat{W}_2,\tilde{b}_{1a}=b_{1a}-\hat{b}_{1a},\ \tilde{b}_{2a}=b_{2a}-\hat{b}_{2a}$. It is obvious that $V>0$ as $s_1\neq 0$ or $s_2\neq 0$ or $\tilde{b}_{1a}\neq 0$ or $\tilde{b}_{2a}\neq 0$. Based on the relation of (B1), we have

$$\tilde{W}_i^T\hat{W}_i=\left\{\left\|\bar{W}_i\right\|^2-\left\|\tilde{W}_i\right\|^2-\left\|\hat{W}_i\right\|^2\right\}/2,\ i=1,2 \quad \text{(B2)}$$

$$\tilde{b}_{1a}\hat{b}_{1a}=\left\{b_{1a}^2-\tilde{b}_{1a}^2-\hat{b}_{1a}^2\right\}/2,\ \tilde{b}_{2a}\hat{b}_{2a}=\left\{b_{2a}^2-\tilde{b}_{2a}^2-\hat{b}_{2a}^2\right\}/2. \quad \text{(B3)}$$

We first consider the case: $\hat{b}_{1a}\ge b_{1al}$ and $\hat{b}_{2a}\ge b_{2al}$. Taking the time derivative of (B1) with suitable relations gives

$$\dot{V}=s_1\dot{s}_1+s_2\dot{s}_2-\tilde{W}_1^T\Gamma_1\dot{\hat{W}}_1-\tilde{W}_2^T\Gamma_2\dot{\hat{W}}_2-\beta_1\tilde{b}_{1a}\dot{\hat{b}}_{1a}-\beta_2\tilde{b}_{2a}\dot{\hat{b}}_{2a}$$
$$=s_1\left\{d_{1a}\left[\ddot{r}_1-\rho_1-b_{1a}u_1-b_4'\eta_1c_7\right]+d_{1v}\left[\dot{r}_1-a_4'-b_4'\eta_1x_7-c_4\right]\right.$$
$$\left.+d_{1p}\left[\dot{r}_1-x_4-c_1\right]+\gamma_1s_1\right\}-\gamma_1s_1^2+s_2\left\{d_{2a}\left[\ddot{r}_3-\rho_2-b_{2a}u_2-b_6'\eta_2c_8\right]\right.$$
$$\left.+d_{2v}\left[\dot{r}_3-a_6'-b_6'\eta_2x_8-c_6\right]+d_{2p}\left[\dot{r}_3-x_6-c_3\right]+\gamma_2s_2\right\}-\gamma_2s_2^2$$
$$-\tilde{W}_1^T\left(s_1\Psi-\alpha_1\hat{W}_1\right)-\tilde{W}_2^T\left(s_2\Psi-\alpha_2\hat{W}_2\right)-\tilde{b}_{1a}\left(s_1\Psi_1-\alpha_3\hat{b}_{1a}\right)$$
$$-\tilde{b}_{2a}\left(s_2\Psi_2-\alpha_4\hat{b}_{2a}\right)=s_1h_1-\left(d_{1a}b_{1a}g_{u_1}-\gamma_1\right)s_1^2-|s_1|d_{1a}b_{1a}g_{u_1}\Delta_1$$
$$-s_1\hat{W}_1^T\Psi b_{1a}/\hat{b}_{1a}+s_2h_2-\left(d_{2a}b_{2a}g_{u_2}-\gamma_2\right)s_2^2-|s_2|d_{2a}b_{2a}g_{u_2}\Delta_2$$
$$-s_2\hat{W}_2^T\Psi b_{2a}/\hat{b}_{2a}-\tilde{W}_1^T\left(s_1\Psi-\alpha_1\hat{W}_1\right)-\tilde{W}_2^T\left(s_2\Psi-\alpha_2\hat{W}_2\right)$$
$$-\tilde{b}_{1a}\left(s_1\Psi_1-\alpha_3\hat{b}_{1a}\right)-\tilde{b}_{2a}\left(s_2\Psi_2-\alpha_4\hat{b}_{2a}\right)-\left(\gamma_1s_1^2+\gamma_2s_2^2\right)$$
$$=s_1\left(\bar{W}_1^T\Psi+\varepsilon_1\right)-s_1\hat{W}_1^T\Psi\left(1+\tilde{b}_{1a}/\hat{b}_{1a}\right)+s_2\left(\bar{W}_2^T\Psi+\varepsilon_2\right)$$
$$-s_2\hat{W}_2^T\Psi\left(1+\tilde{b}_{2a}/\hat{b}_{2a}\right)-\tilde{W}_1^T\left(s_1\Psi-\alpha_1\hat{W}_1\right)-\tilde{W}_2^T\left(s_2\Psi-\alpha_2\hat{W}_2\right)$$
$$-\tilde{b}_{1a}\left(s_1\Psi_1-\alpha_3\hat{b}_{1a}\right)-\tilde{b}_{2a}\left(s_2\Psi_2-\alpha_4\hat{b}_{2a}\right)-\left(d_{1a}b_{1a}g_{u_1}-\gamma_1\right)s_1^2$$
$$-|s_1|d_{1a}b_{1a}g_{u_1}\Delta_1-\left(d_{2a}b_{2a}g_{u_2}-\gamma_2\right)s_2^2-|s_2|d_{2a}b_{2a}g_{u_2}\Delta_2$$
$$-\left(\gamma_1s_1^2+\gamma_2s_2^2\right)\le-\left(d_{1a}b_{1a}g_{u_1}-\gamma_1\right)|s_1|\left\{|s_1|+\Delta_1-|\varepsilon_1|/\left(d_{1a}b_{1a}g_{u_1}-\gamma_1\right)\right\}$$
$$-\left(d_{2a}b_{2a}g_{u_2}-\gamma_2\right)|s_2|\left\{|s_2|+\Delta_2-|\varepsilon_2|/\left(d_{2a}b_{2a}g_{u_2}-\gamma_2\right)\right\}$$
$$+\alpha_1\left\{\left\|\bar{W}_1\right\|^2-\left\|\tilde{W}_1\right\|^2-\left\|\hat{W}_1\right\|^2\right\}/2+\alpha_2\left\{\left\|\bar{W}_2\right\|^2-\left\|\tilde{W}_2\right\|^2-\left\|\hat{W}_2\right\|^2\right\}/2$$
$$+\alpha_3\left\{b_{1a}^2-\tilde{b}_{1a}^2-\hat{b}_{1a}^2\right\}/2+\alpha_4\left\{b_{2a}^2-\tilde{b}_{2a}^2-\hat{b}_{2a}^2\right\}/2-\left(\gamma_1s_1^2+\gamma_2s_2^2\right)$$
$$=-\left(\gamma_1s_1^2+\gamma_2s_2^2\right)-\alpha_1\left\|\tilde{W}_1\right\|^2-\alpha_2\left\|\tilde{W}_2\right\|^2-\alpha_3\tilde{b}_{1a}^2-\alpha_4\tilde{b}_{2a}^2$$
$$-\left(d_{1a}b_{1a}g_{u_1}-\gamma_1\right)F_1\left(|s_1|\right)-\left(d_{2a}b_{2a}g_{u_2}-\gamma_2\right)F_2\left(|s_2|\right)$$
$$+\alpha_1\left\{\left\|\bar{W}_1\right\|^2-\left\|\bar{W}_{1m}\right\|^2-\left\|\hat{W}_1\right\|^2\right\}/2+\alpha_2\left\{\left\|\bar{W}_2\right\|^2-\left\|\bar{W}_{2m}\right\|^2-\left\|\hat{W}_2\right\|^2\right\}/2$$
$$+\alpha_3\left\{b_{1a}^2-b_{1am}^2-\hat{b}_{1a}^2\right\}/2+\alpha_4\left\{b_{2a}^2-b_{2am}^2-\hat{b}_{2a}^2\right\}/2 \quad \text{(B4)}$$

where $F_1\left(|s_1|\right)=|s_1|^2+2f_{11}|s_1|-f_{12},\ F_2\left(|s_2|\right)=|s_2|^2+2f_{21}|s_2|-f_{22}$. The coefficients of the polynomials $F_1\left(|s_1|\right)$ and $F_2\left(|s_2|\right)$ are expressed in (22c). Because $\left\|\bar{W}_i\right\|^2-\left\|\bar{W}_{im}\right\|^2\le 0$, $b_{ia}^2-b_{iam}^2\le 0,\ i=1,2,$ if $F_i\left(|s_i|\right)>0, i=1,2,$ then (B5) is obtained.

$$\dot{V}\le-\mu V \quad \text{(B5)}$$

where $\mu=\min\left\{\min\left[\gamma_1,0.5\right],\min\left[\gamma_2,0.5\right],\min\left[\alpha_1,0.5\lambda\left(\Gamma_1\right)\right],\right.$ $\left.\min\left[\alpha_2,0.5\lambda\left(\Gamma_2\right)\right],\min\left[\alpha_3,0.5\beta_1\right],\min\left[\alpha_4,0.5\beta_2\right]\right\}$. In summary, when $|s_1|>\theta_1$ and $|s_2|>\theta_2$ are obtained (i.e., outside of the domain D_a in (22a)), the closed-loop system possesses the result $\dot{V}\le-\mu V$. Hence, the signal s exponentially converges into the domain D_a (22). Therefore, from (3), (4), (18), (19) and (20) $\left\{s_1,s_2,\tilde{W}_1,\tilde{W}_2,\tilde{b}_{1a},\tilde{b}_{2a}\right\}$ are UUB.

Similarly, the case: $\hat{b}_{1a}<b_{1al}$ and $\hat{b}_{2a}<b_{2al}$ is considered as follows. The difference between these two cases is whether the learning laws (19a) include the projection. Then the time derivative of Lyapunov function becomes the equation (B4) with two extra terms:

$$\dot{V}\le\left[\text{RHS of }(B4)\right]-\alpha_3\tilde{b}_{1a}\left(b_{1al}-\hat{b}_{1a}\right)/\delta_1-\alpha_4\tilde{b}_{2a}\left(b_{2al}-\hat{b}_{2a}\right)/\delta_2. \quad \text{(B6)}$$

Because $0<b_{1al}-\hat{b}_{1a},\ 0<b_{2al}-\hat{b}_{2a},-\tilde{b}_{1a}=-\left(b_{1a}-\hat{b}_{1a}\right)<-\left(b_{1al}-\hat{b}_{1a}\right)$ and $-\tilde{b}_{2a}=-\left(b_{2a}-\hat{b}_{2a}\right)<-\left(b_{2al}-\hat{b}_{2a}\right)$, (B7) becomes more negative than (B4).

$$\dot{V}\le\left[\text{RHS of }(B4)\right]-\alpha_3\left(b_{1al}-\hat{b}_{1a}\right)^2/\delta_1-\alpha_4\left(b_{2al}-\hat{b}_{2a}\right)^2/\delta_2. \quad \text{(B7)}$$

Finally, the same results of the above-mentioned situation: $\hat{b}_{1a}\ge b_{1al}$ and $\hat{b}_{2a}\ge b_{2al}$, is obtained.

Q.E.D.